Received: 22 April 2021 | Revised: 9 August 2021 | Accepted: 9 August 2021

DOI: 10.1002/jcla.23969

RESEARCH ARTICLE

WILEY

Influences of the lncRNA TUG1-miRNA-34a-5p network on fibroblast-like synoviocytes (FLSs) dysfunction in rheumatoid arthritis through targeting the lactate dehydrogenase A (LDHA)

Mei Zhang[1] | Ning Lu[2] | Xiao-Yun Guo[3] | Hong-Jun Li[4] | Ying Guo[1] | Lu Lu[5]

[1]Department of Rheumatology and Immunology, Tianjin Medical University General Hospital, Tianjin, China

[2]Department of Breast Medical Oncology, Tianjin Medical University Cancer Institute and Hospital, National Clinical Research Center for Cancer, Key Laboratory of Cancer Prevention and Therapy, Tianjin's Clinical Research Center for Cancer, Key Laboratory of Breast Cancer Prevention and Therapy, Tianjin Medical University, Ministry of Education, Tianjin, China

[3]Department of Nephrology, The Second Hospital of Tianjin Medical University, Tianjin, China

[4]Department of Rheumatology and Immunology, The Second Hospital of Tianjin Medical University, Tianjin, China

[5]Department of Pharmacy, Tianjin Medical University Cancer Institute and Hospital, National Clinical Research Center for Cancer, Key Laboratory of Cancer Prevention and Therapy, Tianjin's Clinical Research Center for Cancer, Tianjin, China

Correspondence
Mei Zhang, Department of Rheumatology and Immunology, Tianjin Medical University General Hospital, No.154, An-Shan Road, Heping, Tianjin 300052, China.
Email: zhangmeitj@126.com

Funding information
None

Abstract

Background: Rheumatoid arthritis (RA) is a systemic and chronic inflammatory disease. The cellular glucose metabolism of fibroblast-like synoviocytes (FLSs) of RA has been revealed to be essential to the pathogenesis and development of RA. To date, the precise roles and molecular mechanisms of long noncoding RNA TUG1 in RA have not been elucidated.

Methods: TUG1 and miR-34a-5p were detected by qRT-PCR. Interactions between lncRNA-miRNA and miRNA-mRNA were validated by RNA pull-down assay and luciferase assay. The glucose metabolism was evaluated by glucose uptake and extracellular acidification rate (ECAR). Cell viability was determined by MTT assay and Annexin V assay.

Results: TUG1 expression was significantly upregulated in synovial fibroblast-like synoviocytes (FLSs) compared with normal FLSs. Functional assays uncovered that silence of TUG1 suppressed FLSs-RA invasion, migration, glucose metabolism, and increased apoptosis. Bioinformatics analysis indicated that TUG1 interacted with miR-34a-5p. RNA pull-down assay and luciferase assay validated that TUG1 sponged miR-34a-5p in FLSs-RA. Overexpression of miR-34a-5p effectively inhibited glucose metabolism of FLSs-RA. Furthermore, the glucose metabolism of FLSs-RA was significantly elevated compared with normal FLSs. The glucose metabolism enzyme, LDHA, was directly targeted by miR-34a-5p in FLSs. Rescue experiments validated that the miR-34a-5p-inhibited glucose metabolism of FLSs-RA was through targeting LDHA. Finally, we showed restoration of miR-34a-5p in TUG1-overexpressing FLSs-RA successfully overcame the TUG1-promoted glucose metabolism and apoptosis resistance via targeting LDHA.

Conclusion: The present study uncovered critical roles and molecular mechanisms underlying the TUG1-mediated glucose metabolism and apoptosis of FLSs-RA through modulating the miR-34a-5p-LDHA pathway in fibroblast-like synoviocytes of rheumatoid arthritis.

Mei Zhang and Ning Lu Contributed equally.

KEYWORDS
fibroblast-like synoviocytes, glycolysis, miR-34a-5p, rheumatoid arthritis, TUG1

1 | INTRODUCTION

Rheumatoid arthritis (RA) is a systemic autoimmune disease resulting in chronic inflammation, joint destruction, and loss of function.[1] Abnormal synovial hyperplasia is frequently occurred in RA, leading to tissue destruction and functional disability.[2] The proliferative synovial lining tissue which contains a large amount of fibroblast-like synoviocytes (FLSs) is recognized as the main pathological feature of RA.[3] Accumulating evidence revealed that FLSs display an aggressively tumor-like phenotype which contributes to synovial inflammation and cartilage damage.[4] Although therapeutic approaches for RA have improved recently, the side effects and toxicity from the currently available disease-modifying drugs greatly limited the outcomes of RA treatment.[5] Thus, understanding the molecular mechanisms which regulate the biological feathers of FLSs in RA will contribute to developing effectively therapeutic strategies.

Long noncoding RNAs (lncRNAs), which are defined as nonprotein coding transcripts with relative larger size (>200 nucleotides), have been studied as essential regulators for a series of cellular processes, including RA.[6,7] Recent studies identified groups of lncRNAs which were differentially expressed in FLSs-RA compared with healthy donors,[7,8] suggesting lncRNAs are potentially biological targets for RA diagnosis and treatment. The taurine upregulated gene 1 (TUG1) is a novel lncRNA which locates at chromosome 22q12.[9] Increasing evidence indicates that TUG1 participates in the development of diverse cancers, such as colorectal cancer and hepatocellular carcinoma.[10,11] However, the biological roles and mechanism of TUG1 in the pathological progresses of rheumatoid arthritis have not been investigated.

Glucose metabolism shifting toward increased glycolysis is a hallmark of cancer cells which metabolize the majority of glucose into lactate rather than into mitochondrial respiration chain.[12] In addition, cancer cells with dysregulated glycolysis rate exhibit advantages for fast proliferation and anti-apoptosis.[13,14] Recent studies demonstrated that both fibroblasts and activated macrophages display increased glucose consumption rates under and hypoxia and cytokine stimulation.[15,16] Moreover, studies reported the balance between glycolysis and oxidative phosphorylation was shifted toward glycolysis in RA FLSs.[17] The glucose transporter 1 (GLUT1) was detected to be significantly upregulated in FLSs from RA patients,[17] suggesting targeting metabolic pathways could be a novel approach for effective treatment of arthritis through modulating the synoviocyte-mediated inflammation.

In this study, we comprehensively investigated the biologic functions of TUG1 in FLSs from RA. We observed TUG1 was significantly upregulated in FLSs-RA compared with primary normal FLSs. The glucose metabolism of FLSs-RA was remarkedly elevated. Furthermore, the molecular targets of TUG1 in regulating glucose metabolism of FLSs-RA will be identified.

2 | MATERIALS AND METHODS

2.1 | Primary FLS cultures and reagents

The primary normal human FLSs and rheumatoid arthritis (RA) FLSs were purchased from Cell Applications (San Diego, CA, USA). Cells were cultured in DMEM (Thermo Fisher Scientific, Inc., Carlsbad, CA, USA) containing 10% FBS (Bio-Rad, Hercules, CA, USA), 100 units/ml penicillin, and 100 μg/ml streptomycin (Thermo Fisher Scientific, Inc., Carlsbad, CA, USA) at 37°C in a humidified 5% CO_2 atmosphere. Primary synovial cells used in this study were during the passages 3 and 6. Monoclonal rabbit anti-β-actin (#4970) and anti-LDHA (#3582) antibodies were purchased from Cell Signaling Technology (Danvers, MA, USA).

2.2 | Transfections

Transfections were performed using the Lipofectamine 2000 transfection reagent (Invitrogen, Carlsbad, CA, USA) according to the manufacturer's instructions. Briefly, FLSs (4×10^5/well) were seeded onto six-well plates for 24 h. Negative controls, miR-34a-5p or siTUG1, were transfected into FLSs at 25 nM for 48 h. The human LDHA overexpression vector (Myc-DDK-tagged ORF Clone in pCMV6-Entry) was purchased from Origene.com (#RC209378). TUG1 or LDHA overexpression plasmid or control vector was transfected at 1 μg/ml for 48 h using Lipofectamine 2000. Experiments were repeated three times.

2.3 | RNA isolation and real-time PCR

Total RNAs were extracted from cells using the TRIzol reagent (Invitrogen, Carlsbad, CA, USA) according to the manufacturer's instructions. RNA samples were examined using a NanoDrop™ 2000/2000c Spectrophotometers (Thermo Fisher Scientific, Inc., Carlsbad, CA, USA). cDNA was synthesized using 1 μg RNA by using the Revert Aid™ First Strand cDNA Synthesis kit (TaKaRa, Shiga, Japan) according to the manufacturer's instructions. Reactions of qRT-PCR were performed using the Taqman 2X Universal PCR Master Mix (Thermo Fisher Scientific, Inc., Carlsbad, CA, USA). The RT-PCR cycling conditions consisted of 95°C for 10 min; 32 cycle amplification for 30 s at 95°C, 20 s at 55°C, 20 s at 72°C; followed by 1 min at 72°C. U6 was used as an internal control for microRNA

detection. β-Actin was used as an internal control for mRNA and lncRNA detections. The relative expression was calculated using the $2^{-\Delta\Delta Ct}$ method. Experiments were performed in triplicate and repeated three times.

2.4 | Luciferase assay

Luciferase assay was performed using the dual-luciferase assay system (Promega, Madison, WI, USA) according to the manufacturer's instruction. Renilla luciferase was used as an internal control. The wild-type (WT) and mutated (Mut) miR-34a-5p binding sites on TUG1 and 3'-UTR of LDHA were amplified by PCR, followed by cloning into the pMiR-report luciferase vector (Promega, Madison, WI, USA). Cells were co-transfected with control miRNA, miR-34a-5p plus the above constructed luciferase reporter construct using Lipofectamine 3000 (Life Technologies, USA). Experiments were performed in triplicate and repeated three times.

2.5 | RNA pull-down assay

RNA pull-down assay was performed according to previous description.[18] Scramble control, TUG1 sense, and antisense probes were biotin-labeled from RiboBio Co. Ltd (Guangzhou, China). FLS cell lysates were prepared by RIPA buffer followed by incubation with probes for 2 h. Streptavidin-coupled agarose beads (Thermo Fisher Scientific, Shanghai, China) were added into the reactions for 2 h to pull down the RNA-RNA complex. The enrichment of miR-34a-5p in the RNA-RNA complex was determined by qRT-PCR. Experiments were performed in triplicate and repeated three times.

2.6 | Transwell assay

Cell invasive capacity was determined by transwell assay. Chambers (Invitrogen, Waltham, MA, USA) were incubated with cell culture medium (0.5 ml) supplemented with 15% FBS. FLSs (5×10^3) with normal cell culture medium were suspended onto the center of chambers. After 12 h, chambers were collected. Cells on the back of the inserts were fixed by 4% PFA and stained with DAPI. Invaded cells were counted under microscope. Experiments were repeated three times.

2.7 | Measurement of glucose metabolism rate

The glucose uptake and lactate product were detected using the Glucose Uptake Colorimetric Assay Kit (Applygen Technologies, Beijing, China) and Lactate Assay Kit (#MAK064, Sigma, Shanghai, China) according to the manufacturer's instructions. The ECAR was determined using the Seahorse XF Glycolysis Stress Test Kit on a Seahorse XF96e analyzer (Agilent, Santa Clara, CA, USA) according to the manufacturer's instructions. Results were normalized to the cell numbers of each reaction. Experiments were performed in triplicate and repeated three times.

2.8 | Cell viability

FLS cell viability in response to H_2O_2 treatments was examined by MTT assay (Sigma-Aldrich, Shanghai, China) according to the manufacturer's protocols. Briefly, 1×10^3 FLSs per well were seeded into 96-well plate and cultured for 24 h. Post-H_2O_2 treatments protocol, 20-μl MTT (3-(4,5-dimethyl-2-thiazolyl)-2,5-diphenyl-2-H-tetrazolium bromide) was added into each well followed by incubation at 37°C for 4 h. Dimethyl sulfoxide (DMSO) (100 μl) was added into each well to dissolve the formed formazan followed by incubation for 1 h. Absorbance was measured at 570 nm using a SpectraMax M5 microplate reader. Experiments were performed in triplicate and repeated three times.

2.9 | Cell apoptosis assay

Cell apoptosis rate in response to H_2O_2 treatments was examined by Annexin V/FITC Apoptosis Detection Kit I (BD Biosciences, San Jose, CA, USA) according to the manufacturer's protocols. The FLAs-RA or control FLSs (4×10^5/well) were plated on six-well plates and incubated for 24 h. Following treatments, cells were collected and incubated with Annexin V and propidium iodide (PI) for 40 min in a dark environment. The apoptosis rate was evaluated by a FACScan flow cytometer (BD Biosciences). Experiments were performed in triplicate and repeated three times.

2.10 | Western blot

FLSs were collected and lysed by RIPA lysis buffer (Beyotime Biotechnology, Nantong, China) plus 1 × protease inhibitor cocktail (Sigma-Aldrich, Shanghai, China). Lysates were centrifuged at 12,000 g at 4°C for 20 min. Equal amount of protein from each group (40 μg) was loaded onto a 10% SDS-PAGE gel. Proteins were transferred to a nitrocellulose membrane followed by blockading with 5% BSA in TBST buffer. Primary antibodies (1:1000) were incubated with membranes for overnight at 4°C. After complete washing by TBST, membranes were incubated with secondary antibody at room temperature for 2 h. Protein bands were visualized using Hyperfilm-ECL kits (GE Healthcare Biosciences). Experiments were repeated three times.

2.11 | Statistical analysis

Data were displayed as mean ± standard deviation (SD). Statistical analysis was performed using GraphPad Prism 7 software

(GraphPad, La Jolla, CA, USA). The difference between two groups was analyzed by Student's *t* test, and differences among multiple groups were analyzed by one-way analysis of variance (ANOVA) followed by Tukey's test. The linear correlation between TUG1 and miR-34a-5p, miR-34a-5p, and LDHA was analyzed using Spearman's correlation coefficient. $p < 0.05$ was considered to be statistically significant.

3 | RESULTS

3.1 | lncRNA TUG1 is upregulated in human FLSs-RA

Previous studies revealed that FLSs-RA share conventional properties with tumor cells that they displayed tumor-like proliferation, migration, invasion, and resistance to cell death.[4,5] Moreover, lncRNA TUG1 was reported to play oncogenic roles in diverse cancers.[9-11] We therefore evaluated the biological roles of TUG1 in FLSs-RA cells. Expectedly, expression of TUG1 was remarkedly upregulated in human FLSs-RA compared with normal FLSs (Figure 1A). To assess the cellular functions of TUG1 in FLSs-RA, the cell invasion, glucose metabolism, and responses to apoptosis inducer, H_2O_2 was examined in control FLSs or TUG1-silenced FLSs. As we expected, FLSs with lower TUG1 showed significantly suppressed invasion and migration capacity (Figure 1B,C), as well as inhibited glucose metabolism rate (Figure 1D). Importantly, silencing TUG1 effectively sensitized FLSs to apoptosis inducer, H_2O_2 at 500 and 1000 μM for 8 h from cell viability assay and Annexin V apoptosis assay (Figure 1E,F). Taken together, the above results conclude that TUG1 is positively associated with rheumatoid arthritis.

3.2 | LncRNA TUG1 sponges miR-34a-5p to form a ceRNA network in FLSs-RA

To assess the molecular mechanisms underlying the TUG1-mediated glycolysis and cell death of FLSs in RA patients, we searched the potential microRNA targets of TUG1 since it was known that lncRNAs function as miRNAs sponges to block their expressions.[6] Targets prediction from online noncoding RNA service, starBase 2.0, illustrated that miRNA-34a-5p, which has been shown to be negatively associated with cell proliferation of FLSs-RA, contains putative binding sites of TUG1 (Figure 2A). Expectedly, FLSs-RA with lower TUG1 expressions showed significantly upregulated miR-34a-5p expressions (Figure 2B), indicating TUG1 inhibits miR-34a-3p expression via sponging it. Furthermore, RNA pull-down assay concluded that the biotin-labeled antisense RNA probe of TUG1 pulled down enriched miR-34a-5p in FLSs-RA compared with those from scramble and sense RNA probe (Figure 2C). To validate whether TUG1 directly binds with miR-34a-5p, FLSs from RA patients were co-transfected with luciferase vector containing wild-type TUG1 (WT-TUG1) or binding site mutant TUG1 (Mut-TUG1) plus miR-34a-5p or control miRNA. Results showed the luciferase activity of FLSs with co-transfection of WT-TUG1 and miR-34a-5p was significantly inhibited compared with that from the Mut-TUG1 and miRNA-34a-5p co-transfection (Figure 2D). Summarily, these results uncovered that TUG1 downregulates miR-34a-5p via binding it to form a ceRNA network.

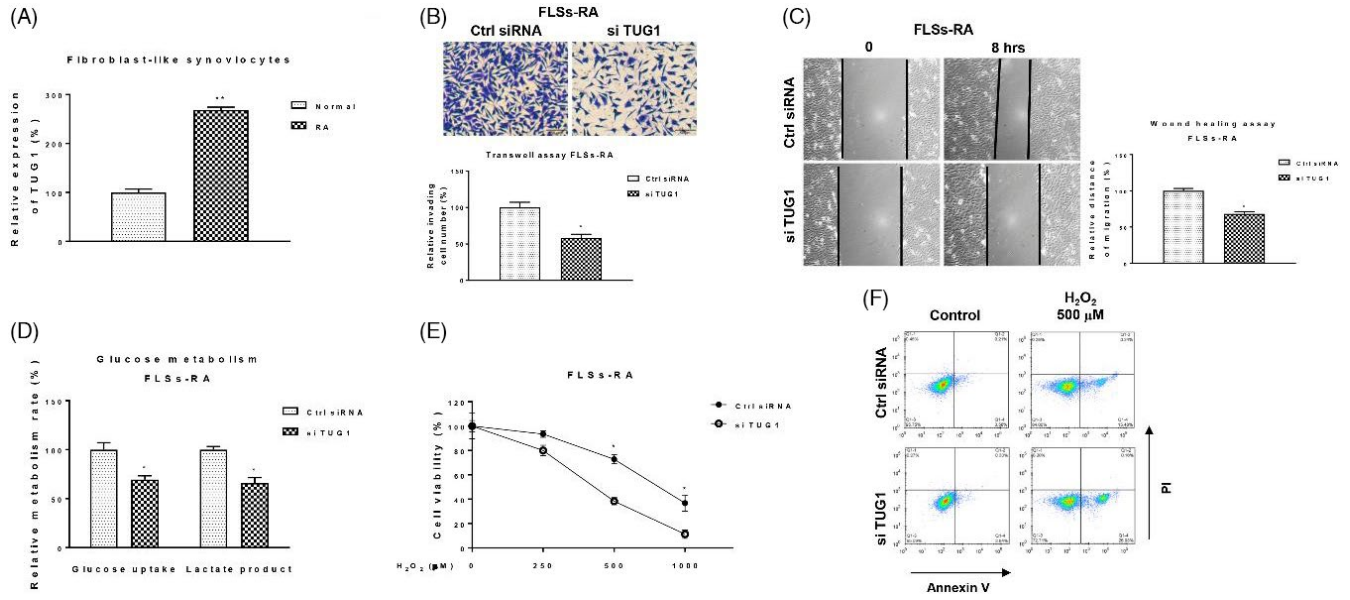

FIGURE 1 TUG1 is positively associated with RA. (A) Expressions of TUG1 were detected by qRT-PCR in primary FLSs from healthy donors and RA patients. (B) FLSs cells from RA patients were transfected with control siRNA or TUG1 siRNA for 48 h, the cell invasion capacity, (C) migration, and (D) glucose metabolism were examined. (E) The above-transfected cells were treated with H_2O_2 at 0, 250, 500, or 1000 μM for 8 h; the cell viability was determined by MTT and (F) Annexin V apoptosis assay. $^*p < 0.05$; $^{**}p < 0.01$

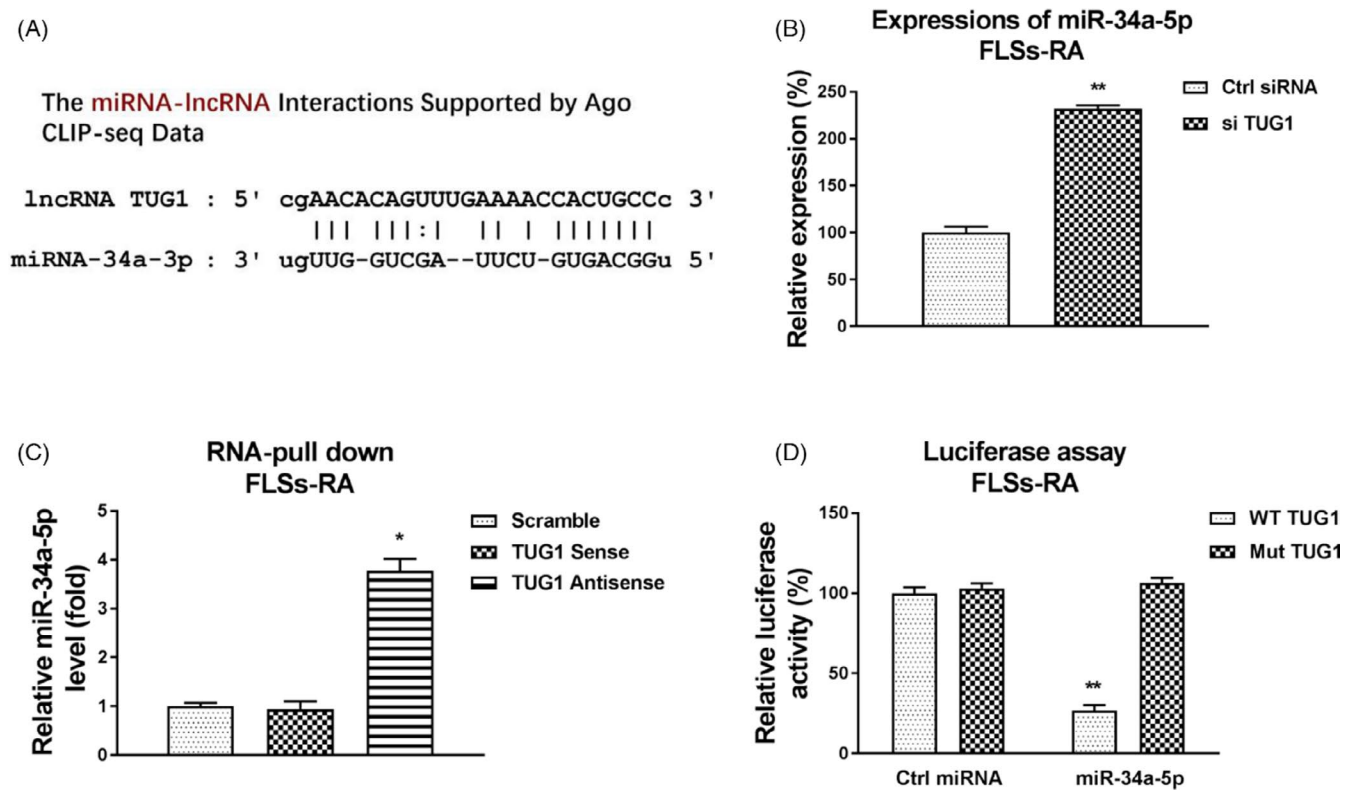

FIGURE 2 TUG1 downregulates miR-34a-5p via sponging as a ceRNA. (A) Prediction of TUG1-miR-34a-5p interaction from StarBase. (B) FLSs-RA was transfected with control siRNA or TUG1 siRNA for 48 h; expressions of miR-34a-5p were detected by qRT-PCR. (C) FLSs-RA cell lysates were incubated with scramble control, biotin-labeled TUG1 sense, or antisense probe for biotin pull-down assay. The enrichment of miR-34a-5p was assessed by qRT-PCR. (D) Dual-luciferase reporter assay was performed by transfection of WT-TUG1 or Mut-TUG1 luciferase vector with control miRNA or miR-34a-5p into FLSs-RA. Luciferase activities were detected. $^{*}p < 0.05$; $^{**}p < 0.01$

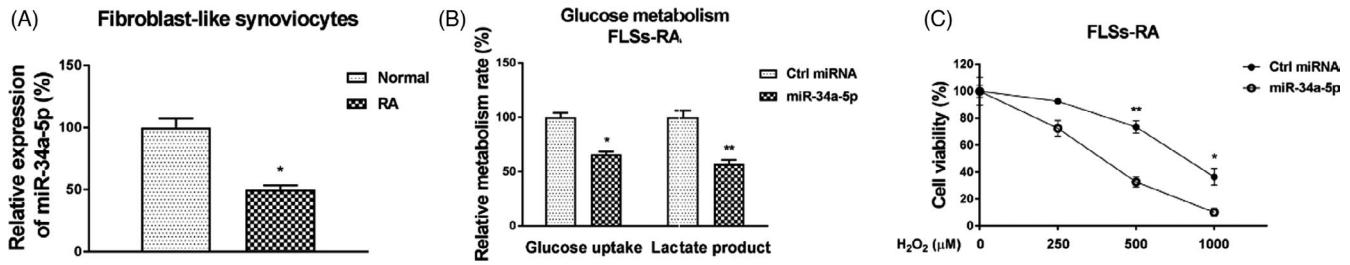

FIGURE 3 miR-34a-5p is negatively associates with RA. (A) Expressions of miR-34a-5p were detected by qRT-PCR in isolated FLSs from healthy donors and RA patients. (B) FLSs cells from RA patients were transfected with control miRNA or miR-34a-5p for 48 h; glucose uptake and lactate product were examined. (C) The above-transfected cells were treated with H_2O_2 at 0, 250, 500, or 1000 μM for 8 h; the cell viability was determined by MTT assay. $^{*}p < 0.05$; $^{**}p < 0.01$

3.3 | miR-34a-5p inhibits glycolysis rate and induces cell death of FLSs-RA

Since we have shown the positive roles of TUG1 in FLSs-RA and the TUG1-miR-34a-5p interaction, we then hypothesized miR-34a-5p plays negative roles in FLSs-RA. Expressions of miR-34a-5p were remarkedly attenuated in human FLSs-RA compared with normal FLSs (Figure 3A). Consequently, the cellular functions of miR-34a-5p were assessed. Consistently, FLSs-RA with miR-34a-5p overexpression showed effectively inhibited glucose metabolism rate (Figure 3B). Overexpression of miR-34a-5p significantly blocked the glucose uptake and lactate product of FLSs-RA (Figure 3B). Furthermore, FLSs with miR-34a-5p overexpression showed significantly increased apoptosis rate (Figure 3C). In summary, these results revealed that miR-34a-5p is negatively associated with glucose metabolism and promotes apoptosis of FLSs-RA.

3.4 | Glucose metabolism is elevated in FLSs from RA

To investigate the effects of the miR-34a-5p-suppressed glucose metabolism on FLSs-RA, the glucose uptake and ECAR were examined in FLSs from normal tissue and RA tissue. As we expected, compared

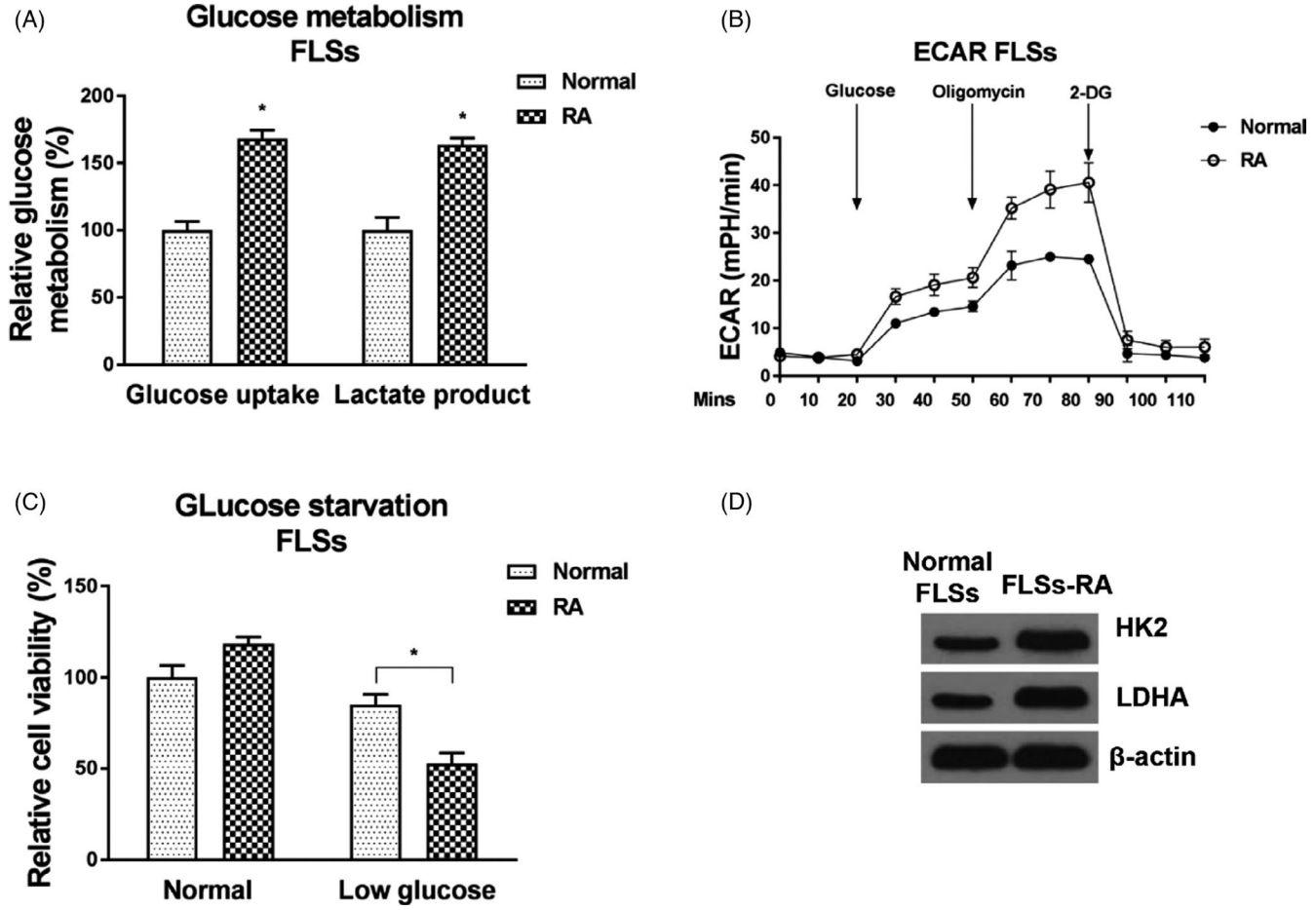

FIGURE 4 Glutamine metabolism rate is elevated in FLSs-RA. (A) Glucose uptake, lactate product, and (B) extracellular acidification rate were examined in FLSs from normal and RA patients. (C) FLSs from normal and RA patients were cultured under normal or low glucose condition; the cell viability was examined by MTT assay. (D) The glycolysis enzymes, HK2, and LDHA were detected by Western blot in FLSs from normal and RA patients. β-Actin was an internal control. $^{**}p < 0.01$

to healthy FLSs, the glycolysis rates of FLSs-RA were significantly elevated (Figure 4A,B). Under low glucose supply, FLSs-RA displayed inhibited cell viability compared with that from healthy FLSs (Figure 4C), suggesting FLSs-RA exhibit a glucose addictive characteristic. Consistently, the mRNA expressions of hexokinase 2 (HK2) and LDHA were apparently upregulated in FLSs-RA (Figure 4D). These results suggest that targeting the dysregulated glycolysis of FLSs-RA could be an effective strategy for RA treatment.

3.5 | miR-34a-5p targets LDHA to inhibit glycolysis of FLSs-RA

Given that microRNAs directly bind to the 3'UTR of target mRNAs to interfere their transcriptions,[19] we examined the molecular targets of miR-34a-5p by searching the noncoding RNA service, starBase.org. Among all predicted targets, LDHA, which catalyzes the conversion of pyruvate to lactate of anaerobic glycolysis,[20] was observed to contain putative miR-34a-5p binding sites on its 3'UTR (Figure 5A). In addition, LDHA mRNA was detected to be significantly upregulated in RA synovial cells compared with normal synovial cells (Figure 5B). Expectedly, silencing LDHA by siRNA effectively sensitized FLSs-RA cells to H_2O_2 treatments compared with control siRNA transfection (Figure 5C). To examine whether LDHA could be downregulated by miR-34a-5p, miR-34a-5p was overexpressed in FLSs-RA. Western blot results showed overexpression of miR-34a-5p remarkedly blocked LDHA protein expression (Figure 5D). To validate whether miR-34a-5p directly targets the 3′UTR of LDHA, luciferase reporter assays were performed by co-transfection of luciferase vector containing wild type- or binding site mutant-3′UTR of LDHA with control miRNA or miR-34a-5p into FLSs-RA and normal FLSs. Expected luciferase assay demonstrated that overexpression of miR-34a-5p significantly suppressed the luciferase activity of WT-LDHA 3′-UTR but not that from the Mut-LDHA 3′-UTR (Figure 5E,F). Together, these results consistently demonstrated that miR-34a-5p directly targets 3′UTR of LDHA in FLSs.

3.6 | Restoration of LDHA rescues the miR-34a-5p-inhibited glycolysis and FLSs-RA apoptosis

To assess whether the miR-34a-5p-mediated glycolysis inhibition and FLSs-RA apoptosis were through targeting LDHA, functional

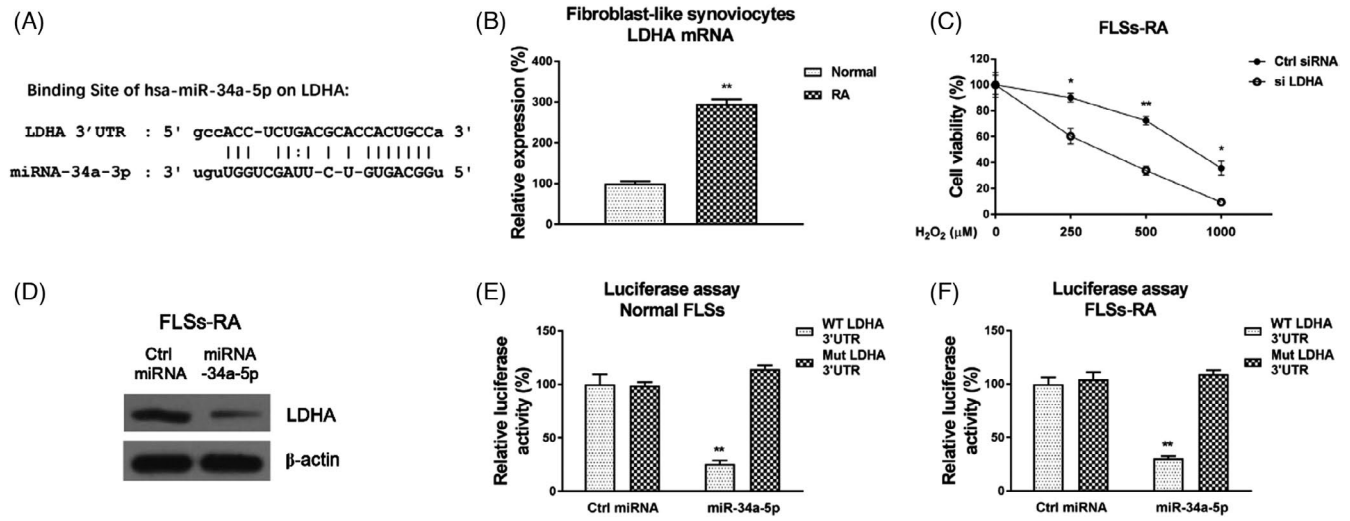

FIGURE 5 miR-34a-5p directly targets 3′UTR of LDHA in FLSs. (A) Prediction of the miR-34a-5p binding sites on 3′UTR of LDHA from StarBase. (B) Expressions of LDHA were detected by qRT-PCR in normal FLSs and FLSs-RA. (C) FLSs cells from RA patients were transfected with control siRNA or LDHA siRNA for 48 h; cells were treated with H_2O_2 at the indicated concentrations. Cell viability was examined by MTT assay. (D) FLSs from RA patients were transfected with control miRNA or miR-34a-5p; protein expressions of LDHA were detected by Western blot. (E) Dual-luciferase reporter assay was performed by transfection of WT- or Mut-3'UTR of LDHA with control miRNA or miR-34a-5p into normal FLSs and (F) FLSs-RA. Luciferase activities were detected. $^*p < 0.05$; $^{**}p < 0.01$

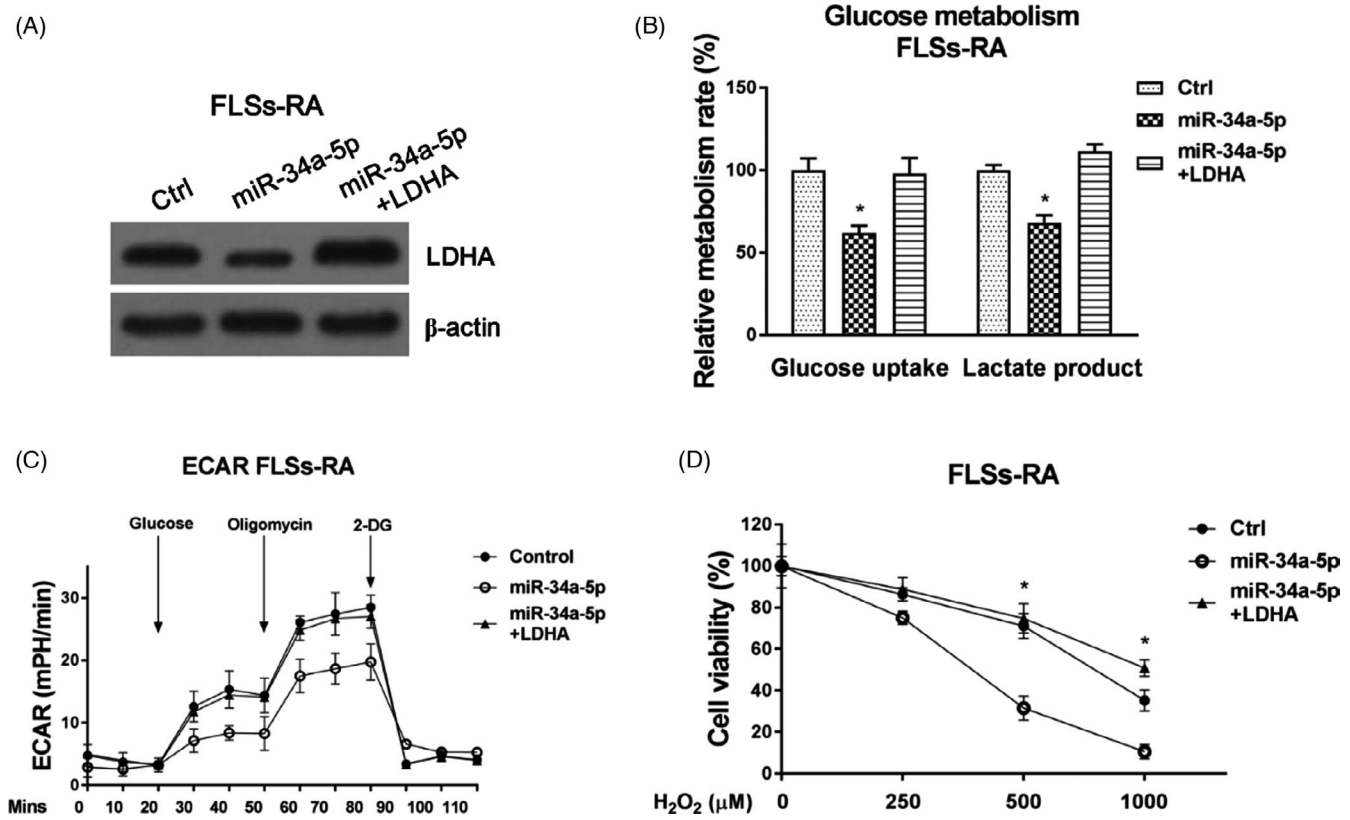

FIGURE 6 Restoration of LDHA rescues the miR-34a-5p-mediated glycolysis and apoptosis in FLSs-RA. (A) FLSs-RA were transfected with control (negative control miRNA plus empty vector), miR-34a-5p alone, or combined with LDHA for 48 h, expressions of LDHA were detected by Western blot. (B) Glucose uptake and (C) ECAR were detected from the above-transfected cells. (D) The above-transfected cells were treated with H_2O_2 at the indicated concentrations for 8 h; cell viability was determined by MTT assay. $^*p < 0.05$; $^{**}p < 0.01$

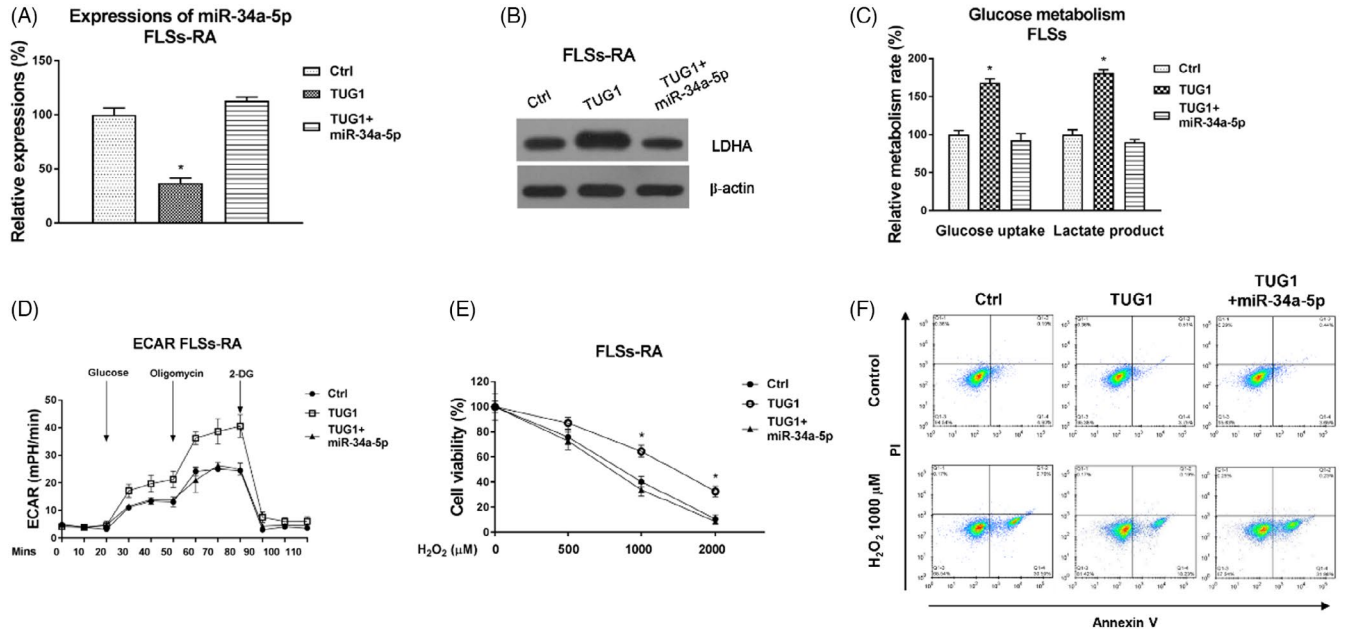

FIGURE 7 Roles of TUG1-miR-34a-5p-LDHA axis in FLSs-RA. (A) FLSs-RA was transfected with control, TUG1 alone, or combined with miR-34a-5p for 48 h, miR-34a-5p and (B) protein expressions of LDHA were examined by qRT-PCR and Western blot, respectively. (C) Glucose uptake assay and (D) ECAR were measured from the above-transfected cells. (E) FLSs-RA were transfected with control, TUG1 alone or combined with miR-34a-5p for 48 h, cells were treated with H_2O_2 at the indicated concentrations for 48 h, and cell viability was determined by MTT assay and (F) Annexin V apoptosis assay. $^*p < 0.05$; $^{**}p < 0.01$

rescue experiments were performed by transfection of control miRNA, miR-34a-5p alone or plus LDHA overexpression plasmid into FLSs-RA. Western blot results showed transfection of LDHA in miR-34a-5p overexpressing FLSs-RA successfully recovered the LDHA protein expression (Figure 6A). Moreover, restoration of LDHA effectively rescued the glucose uptake, lactate product, and ECAR (Figure 6B,C). Importantly, FLSs-RA with recovered LDHA exhibited decreased cell sensitivity to apoptosis inducer from cell viability assay (Figure 6D). In summary, the above results consistently demonstrated that miR-34a-5p suppressed glucose metabolism and increased apoptosis of FLSs-RA via direct targeting LDHA.

3.7 | LncRNA TUG1 attenuates apoptosis of FLSs-RA via the miR-34a-5p-LDHA axis

We then asked whether the TUG1 affects the H_2O_2-induced FLSs-RA apoptosis through modulating the miR-34a-5p-LDHA-glycolysis axis. Negative control, TUG1 overexpression vector alone or plus miR-34a-5p was transfected into FLSs-RA. qPCR results from Figure 7A demonstrated overexpression of TUG1 suppressed miR-34a-5p, which could be further rescued by miR-34a-5p transfection. In addition, Western blot results showed that overexpression or silencing of TUG1 significantly upregulated or inhibited LDHA expression, respectively (Figure 7B, Figure S1). Consequently, the TUG1-upregulated LDHA was effectively blocked by miR-34a-5p transfection (Figure 7B). Furthermore, rescue of miR-34a-5p in TUG1-overexpressing FLSs-RA remarkedly re-suppressed glucose uptake, lactate product, and ECAR (Figure 7C,D) and increased the apoptosis (Figure 7E,F). Taken together, these data validated that TUG1 blocked the H_2O_2-induced FLSs-RA apoptosis by modulating the miR-34a-5p-LDHA axis, presenting TUG1 as a biomarker and molecular target for the diagnosis and treatment of rheumatoid arthritis.

4 | DISCUSSION

Rheumatoid arthritis (RA) is a chronic inflammatory joint disease with synovial inflammation.[1,2] Fibroblast-like synoviocytes (FLSs), which are the major cell population in synovial tissues, play vital roles in the initiation and progressions of the immune response in patients with RA.[3] Hyper-proliferative FLSs have the increased capacities to migrate into articular cartilage and secrete diverse pro-inflammatory cytokines, leading to exacerbation of RA progressions.[3] This study aimed to investigate the biological roles and mechanisms of lncRNA-TUG1 in the cellular metabolism and the oxidative stress-induced cell dysfunction of FLSs-RA. In the present study, for the first time, we showed that FLSs from RA exhibited significantly upregulated TUG1 expressions compared with normal FLSs, suggesting TUG1 could be a diagnostic biomarker and therapeutic target against RA.

Growing evidence indicated that FLSs of RA patients exhibit aggressively cancer-like features, including fast proliferation, increased migratory and invasive capacities, and resistance to apoptosis.[4,5] The dysregulated bioactivities of FLSs-RA largely contribute to joint cartilage and bone destruction.[5] A number of lncRNAs have been demonstrated to contribute to the pathogenesis of disease,

especially cancer.[6] Moreover, a lncRNA microarray analysis between FLSs-RA and healthy control revealed a large amount of differentially expressed lncRNAs in FLSs-RA,[7,8] indicating lncRNAs play vital roles in the pathogenesis and progress of RA. TUG1 was reported to be positively associated with multiple cancers. Here, we demonstrate TUG1 promotes cellular glucose metabolism and decreased apoptosis of FLSs-RA, consistent with the oncogenic roles of TUG1 in cancers.

It was widely studied that lncRNAs acted as sponges of target miRNAs to downregulate their expressions, leading to de-repression of miRNA targets.[21] By luciferase assay and RNA pull-down assay, we identified miR-34a-5p, which acts as a tumor suppressor in cancers, was suppressed by TUG1 in FLSs-RA via forming a ceRNA network with TUG1. Subsequently, we identified the glucose metabolism key enzyme, LDHA as a direct target of miR-34a-5p in FLSs-RA. Rescue experiments clearly validated the miR-34a-5p-mediated glucose metabolism inhibition and apoptosis of FLSs-RA was through direct targeting LDHA. In addition, restoration of miR-34a-5p in TUG1-overexpressing FLSs-RA effectively overcame the TUG1-promoted glucose metabolism and anti-apoptosis phenotypes.

Similar to cancer cells, FLSs-RA display increased glucose consumption rate and metabolic shift toward increased anaerobic glycolysis from mitochondrial phosphorylation.[15-17] This study revealed TUG1 functions as a glycolysis promoter of FLSs-RA. In addition, under low glucose condition, FLSs-RA displayed increased apoptosis compared with normal FLSs, suggesting blocking the TUG1-promoted glucose metabolism pathway could be an effective approach against RA. Although the TUG1-miR34a-5p and miR-34a-5p-LDHA axis have been evaluated in cancers,[22-24] our study for the first time integrated it into the TUG1-mediated phenotypes of FLSs-RA. However, this study still has limitations that the above in vitro molecular signaling pathway needs to be validated by in vivo experiments.

In summary, our conclusions uncover critical roles and molecular mechanisms of the TUG1-mediated glucose metabolism and apoptosis of FLSs-RA through modulating the miR-34a-5p-LDHA pathway in RA patients, suggesting that targeting TUG1 could be an effective therapeutic approach to suppress the proliferation of FLSs for rheumatoid arthritis treatment.

ACKNOWLEDGEMENT

None.

CONFLICTS OF INTEREST

The authors declared no potential conflicts of interest.

AUTHOR CONTRIBUTIONS

M.Z and N.L. designed the experiments. X.Y.G., H.J.L., Y.G., and L.L. carried out the experiments and analyzed the data. All authors participated in the manuscript preparation.

DATA AVAILABILITY STATEMENT

The data that support the findings of this study are available from the corresponding author upon reasonable request.

ORCID

Mei Zhang https://orcid.org/0000-0002-1543-4253

REFERENCES

1. Croia C, Bursi R, Sutera D, Petrelli F, Alunno A, Puxeddu I. One year in review 2019: pathogenesis of rheumatoid arthritis. *Clin Exp Rheumatol*. 2019;37(3):347-357.
2. McInnes IB, Schett G. The pathogenesis of rheumatoid arthritis. *N Engl J Med*. 2011;365(23):2205-2219.
3. Karami J, Aslani S, Tahmasebi MN, et al. Epigenetics in rheumatoid arthritis; fibroblast-like synoviocytes as an emerging paradigm in the pathogenesis of the disease. *Immunol Cell Biol*. 2020;98(3):171-186.
4. Morand S, Staats H, Creeden JF, et al. Molecular mechanisms underlying rheumatoid arthritis and cancer development and treatment. *Future Oncol*. 2020;16(9):483-495.
5. Jayashree S, Nirekshana K, Guha G, Bhakta-Guha D. Cancer chemotherapeutics in rheumatoid arthritis: a convoluted connection. *Biomed Pharmacother*. 2018;102:894-911.
6. Kopp F, Mendell JT. Functional classification and experimental dissection of long noncoding RNAs. *Cell*. 2018;172(3):393-407.
7. Liang J, Chen W, Lin J. LncRNA: an all-rounder in rheumatoid arthritis. *J Transl Inter Med*. 2019;7(1):3-9.
8. Wang J, Yan S, Yang J, Lu H, Xu D, Wang Z. Non-coding RNAs in rheumatoid arthritis: from bench to bedside. *Front Immunol*. 2019;10:3129.
9. Zhou H, Sun L, Wan F. Molecular mechanisms of TUG1 in the proliferation, apoptosis, migration and invasion of cancer cells. *Oncol Lett*. 2019;18(5):4393-4402.
10. Shen X, Hu X, Mao J, et al. The long noncoding RNA TUG1 is required for TGF-β/TWIST1/EMT-mediated metastasis in colorectal cancer cells. *Cell Death Dis*. 2020;11(1):65.
11. Lin YH, Wu MH, Huang YH, et al. Taurine up-regulated gene 1 functions as a master regulator to coordinate glycolysis and metastasis in hepatocellular carcinoma. *Hepatology*. 2018;67(1):188-203.
12. Ganapathy-Kanniappan S. Molecular intricacies of aerobic glycolysis in cancer: current insights into the classic metabolic phenotype. *Crit Rev Biochem Mol Biol*. 2018;53(6):667-682.
13. Abbaszadeh Z, Çeşmeli S, Biray AÇ. Crucial players in glycolysis: cancer progress. *Gene*. 2020;726:144158.
14. Akins NS, Nielson TC, Le HV. Inhibition of glycolysis and glutaminolysis: an emerging drug discovery approach to combat cancer. *Curr Top Med Chem*. 2018;18(6):494-504.
15. Bustamante MF, Garcia-Carbonell R, Whisenant KD, Guma M. Fibroblast-like synoviocyte metabolism in the pathogenesis of rheumatoid arthritis. *Arthritis Res Ther*. 2017;19(1):110.
16. Bustamante MF, Oliveira PG, Garcia-Carbonell R, et al. Hexokinase 2 as a novel selective metabolic target for rheumatoid arthritis. *Ann Rheum Dis*. 2018;77(11):1636-1643.
17. Garcia-Carbonell R, Divakaruni AS, Lodi A, et al. Critical role of glucose metabolism in rheumatoid arthritis fibroblast-like synoviocytes. *Arthritis Rheum*. 2016;68(7):1614-1626.
18. Torres M, Becquet D, Guillen S, et al. RNA pull-down procedure to identify RNA targets of a long non-coding RNA. *J Vis Exp*. 2018;134.
19. Rupaimoole R, Slack FJ. MicroRNA therapeutics: towards a new era for the management of cancer and other diseases. *Nat Rev Drug Discovery*. 2017;16(3):203-222.
20. Feng Y, Xiong Y, Qiao T, Li X, Jia L, Han Y. Lactate dehydrogenase A: a key player in carcinogenesis and potential target in cancer therapy. *Cancer Med*. 2018;7(12):6124-6136.
21. Paraskevopoulou MD, Hatzigeorgiou AG. Analyzing MiRNA-LncRNA interactions. *Methods Mol Biol*. 2016;1402:271-286.
22. Liu L, Chen X, Zhang Y, Hu Y, Shen X, Zhu W. Long non-coding RNA TUG1 promotes endometrial cancer development via inhibiting miR-299 and miR-34a-5p. *Oncotarget*. 2017;8(19):31386-31394.

23. Zhang Y, Zhao D, Li S, et al. Long non-coding RNA TUG1 knockdown hinders the tumorigenesis of multiple myeloma by regulating the microRNA-34a-5p/NOTCH1 signaling pathway. *Open Life Sci*. 2020;15(1):284-295.
24. Zhang L, Fu Y, Guo H. c-Myc-induced long non-coding RNA small nucleolar RNA host gene 7 regulates glycolysis in breast cancer. *J Breast Cancer*. 2019;22(4):533-547.

SUPPORTING INFORMATION

Additional supporting information may be found online in the Supporting Information section.

How to cite this article: Zhang M, Lu N, Guo X-Y, Li H-J, Guo Y, Lu L. Influences of the lncRNA TUG1-miRNA-34a-5p network on fibroblast-like synoviocytes (FLSs) dysfunction in rheumatoid arthritis through targeting the lactate dehydrogenase A (LDHA). *J Clin Lab Anal*. 2021;35:e23969. https://doi.org/10.1002/jcla.23969